

Aspects of Dark Energy Universe with Barboza Alcaniz Zhu and Silva Redshift Parameterization

Promila Biswas,
Department of Mathematics
The University of Burdwan
“Cosmology from Home 2021”

June 22, 2021

- 1 Introduction
- 2 Mathematical Constructions
- 3 Data Analysis
- 4 Behaviours of Cosmological Parameters
- 5 Brief Conclusions and Discussions
- 6 References

Cosmic Acceleration : Reverting back Λ

To justify the cosmic acceleration, Einsteins equation was modified.

Cosmic Acceleration : Reverting back Λ

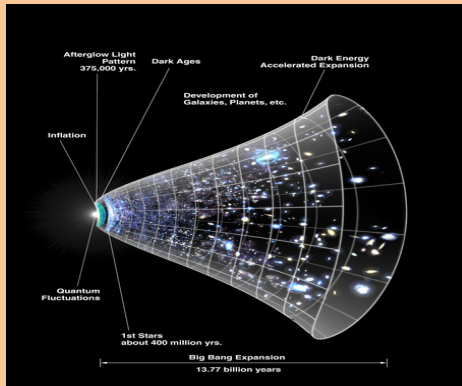
To justify the cosmic acceleration, Einsteins equation was modified. Modification of the left hand side ($G_{\mu\nu}$) led to modified gravity theories and the right hand sides ($T_{\mu\nu}$) modification gave us the idea of exotic matters like dark energies.

Cosmic Acceleration : Reverting back Λ

To justify the cosmic acceleration, Einsteins equation was modified. Modification of the left hand side ($G_{\mu\nu}$) led to modified gravity theories and the right hand sides ($T_{\mu\nu}$) modification gave us the idea of exotic matters like dark energies. However, Einsteins cosmological constant is seemed to be fit till date.

What is Dark Energy & How it permeates all the Cosmos?

Dark Energy is a mysterious repulsive force seems to dominate the Cosmos and it permeates all the cosmos, exerting negative pressure to accelerate the expansion of the universe. 68% of the universe is dark energy. Dark matter makes up about 27%. The rest - everything on earth is less than 5% of the universe.



Credit : thesciencegreek.org

Motivation of our work

- We want to study the natures of Barboza Alcaniz Zhu and Silva redshift parameterization [1] dark energy model. We constrain the free parameters of the model under differential ages data.
- We want to show the fractional dimensionless density parameter for this dark energy model either grows up with time or starts to dominate that of matter since recent past.
- We want to find out some cases where future deceleration takes place. We analyse the space of statefinder parameters [2].

Equation of state of Barboza, Alcaniz, Zhu and Silva [1] given as

$$\omega_d = \omega_0 - \omega_1 \frac{(1+z)^{-\beta} - 1}{\beta} .$$

Basic Calculations

We will use the conservation equation,

$$\dot{\rho} + 3H(\rho + p) = 0 \quad . \quad (1)$$

We get solving (1) for our dark energy model,

$$\rho_d(z) = \rho_{d_0}(1+z)^{\frac{3\{\omega_1+\beta(1+\omega_0)\}}{\beta}} \exp \left[\frac{3\omega_1}{\beta^2} \{(1+z)^{-\beta} - 1\} \right] \quad (2)$$

Finally combining, $\rho_{tot} = \rho_{rad} + \rho_m + \rho_d$

$$= \rho_{rad_0}(1+z)^4 + \rho_{m_0}(1+z)^3 + \rho_{d_0}(1+z)^{\frac{3\{\omega_1+\beta(1+\omega_0)\}}{\beta}} \exp \left[\frac{3\omega_1}{\beta^2} \{(1+z)^{-\beta} - 1\} \right] \quad . \quad (3)$$

We consider FLRW universe where Einstein's field equations turn to be,

$$\left(\frac{\dot{a}}{a}\right)^2 + \frac{kc^2}{a^2} = \frac{8\pi G}{3}\rho_{tot}$$

and
$$\frac{2\ddot{a}}{a} + \left(\frac{\dot{a}}{a}\right)^2 + \frac{kc^2}{a^2} = -\frac{8\pi G}{c^2}p_{tot}.$$

So, we write Hubble's parameter as redshift's function for flat space,

$$H^2 = H_0^2 \left[\Omega_{rad_0}(1+z)^4 + \Omega_{m_0}(1+z)^3 + \right.$$

$$\left. \Omega_{d_0}(1+z)^{\frac{3\{\omega_1+\beta(1+\omega_0)\}}{\beta}} \exp \left[\frac{3\omega_1}{\beta^2} \{(1+z)^{-\beta} - 1\} \right] \right] \quad (4)$$

where $\Omega_{i_0} = \frac{8\pi G}{3H_0^2}\rho_{i_0}$, $i = rad, m, d$ represent dimensionless fractional density parameters related to radiation, matter and dark energy respectively.

The definition of chi-square as $\chi^2 = \sum \frac{\{H_{obs} - H(z)\}^2}{\sigma^2(z)}$.

BAO peak parameter [3] is defined as $\mathcal{A}_{BAO} = \frac{\sqrt{\Omega_m}}{E(z_1)^{\frac{1}{3}}} \left\{ \frac{1}{z_1} \int_0^{z_1} E(z)^{-1} dz \right\}^{\frac{2}{3}}$

and for flat FLRW model, the value of \mathcal{A}_{BAO} is turned to be 0.469 ± 0.017 . So modified chi-squared becomes,

$$\chi_{BAO}^2 = \frac{(\mathcal{A}_{BAO} - 0.469)^2}{0.017^2} . \quad (5)$$

Shift parameter for CMB power spectrum peak [4] looks like

$$\mathcal{R} = \sqrt{\Omega_m} \int_0^{z_2} \frac{dz'}{E(z')}$$

$$\chi_{CMB}^2 = \frac{(\mathcal{R} - 1.726)^2}{0.018^2} . \quad (6)$$

Constraining ω_1 and ω_2 with different values of constant β

fig.1(a)

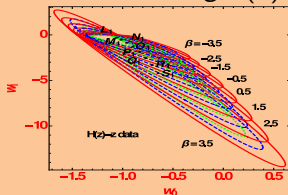


fig.1(b)

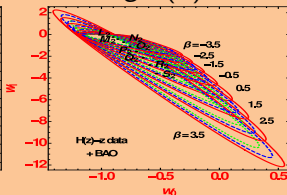
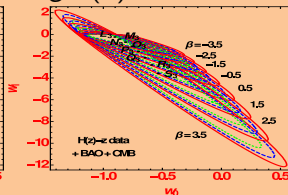


fig.1(c)



- If β is highly positive, low ω_1 value is supported with high ω_0 values and vice versa.

Constraining ω_1 and ω_2 with different values of constant β

fig.1(a)

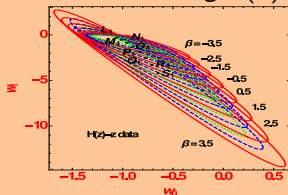


fig.1(b)

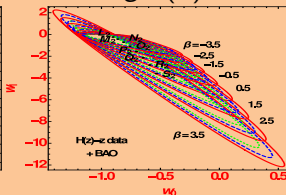
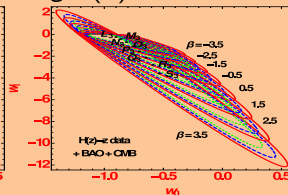
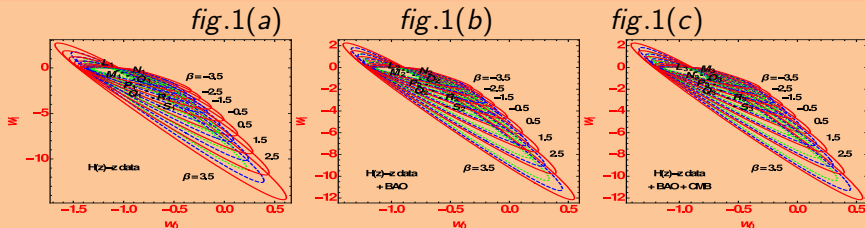


fig.1(c)



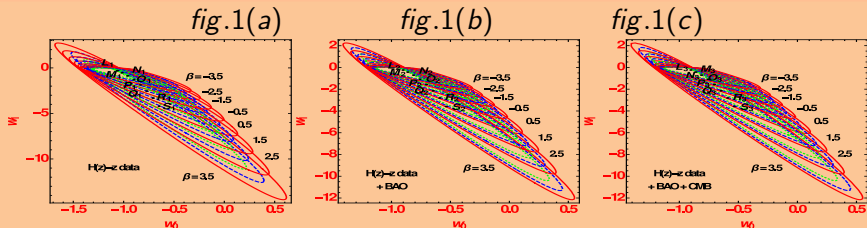
- If β is highly positive, low ω_1 value is supported with high ω_0 values and vice versa.
- If $\beta_1 > \beta_2$ then $\theta_{\beta_1} < \theta_{\beta_2}$. However if $\beta_1 > \beta_2$ the span of the confidence contours for the second case is smaller than first one.

Constraining ω_1 and ω_2 with different values of constant β



- If β is highly positive, low ω_1 value is supported with high ω_0 values and vice versa.
- If $\beta_1 > \beta_2$ then $\theta_{\beta_1} < \theta_{\beta_2}$. However if $\beta_1 > \beta_2$ the span of the confidence contours for the second case is smaller than first one.
- It is observed that $\omega(z=0) = \omega_0$ is perfectly matches with present day observational data when $\beta < 0.5$.

Constraining ω_1 and ω_2 with different values of constant β



- If β is highly positive, low ω_1 value is supported with high ω_0 values and vice versa.
- If $\beta_1 > \beta_2$ then $\theta_{\beta_1} < \theta_{\beta_2}$. However if $\beta_1 > \beta_2$ the span of the confidence contours for the second case is smaller than first one.
- It is observed that $\omega(z=0) = \omega_0$ perfectly matches with present day observational data when $\beta < 0.5$.
- When BAO and CMB tools are applied along with the $H(z) - z$ data, negativeness of EoS at present epoch is reduced.

Constraining all the Parameters with Combined/ Upgraded tools

fig.2(a)

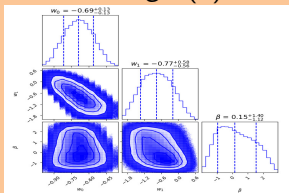


fig.2(b)

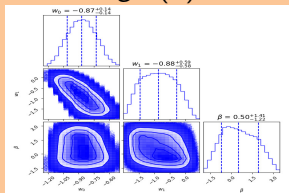
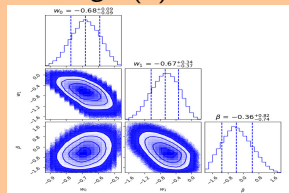


fig.2(c)



- If BAO constrain is working with the Hubble parameter data, this model supports Λ CDM within its one sigma confidence.

Constraining all the Parameters with Combined/ Upgraded tools

fig.2(a)

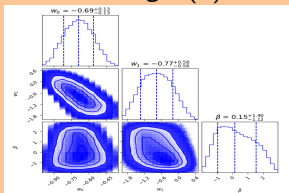


fig.2(b)

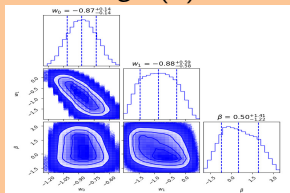
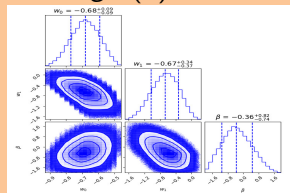


fig.2(c)



- If BAO constrain is working with the Hubble parameter data, this model supports Λ CDM within its one sigma confidence.
- Hubble parameter data equipped with BAO constraints together maximally reaches upto a value of $EoS = -0.87^{+0.14}_{-0.14}$ at present time and adding with it CMB tools it reaches up to $-0.68^{+0.09}_{-0.09}$.

Constraining all the Parameters with Combined/ Upgraded tools

fig.2(a)

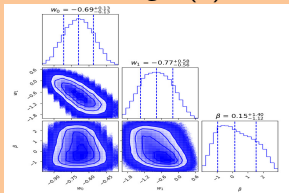


fig.2(b)

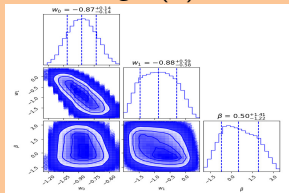
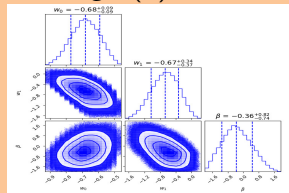


fig.2(c)



- If BAO constrain is working with the Hubble parameter data, this model supports Λ CDM within its one sigma confidence.
- Hubble parameter data equipped with BAO constraints together maximally reaches upto a value of $EoS = -0.87^{+0.14}_{-0.14}$ at present time and adding with it CMB tools it reaches up to $-0.68^{+0.09}_{-0.09}$.
- Variations of w_0 and w_1 are almost symmetric.

Constraining all the Parameters with Combined/ Upgraded tools

fig.2(a)

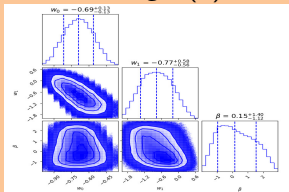


fig.2(b)

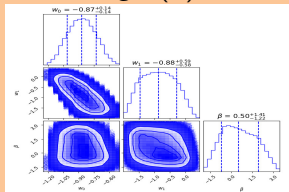
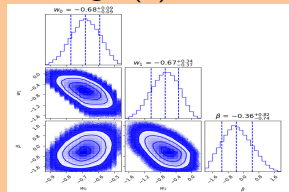
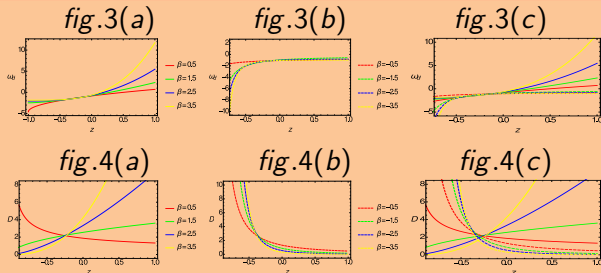


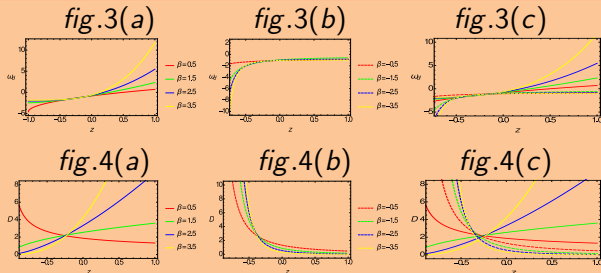
fig.2(c)



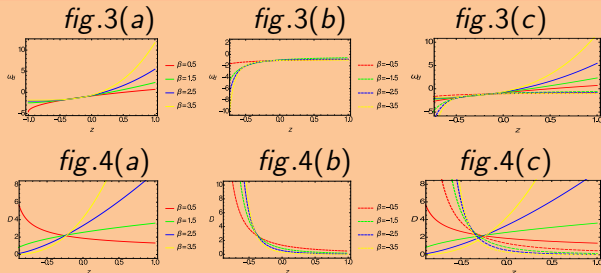
- If BAO constrain is working with the Hubble parameter data, this model supports Λ CDM within its one sigma confidence.
- Hubble parameter data equipped with BAO constraints together maximally reaches upto a value of $EoS = -0.87^{+0.14}_{-0.14}$ at present time and adding with it CMB tools it reaches up to $-0.68^{+0.09}_{-0.09}$.
- Variations of w_0 and w_1 are almost symmetric.
- β is observed to be negatively skewed and found to vary through a long range though.

EoS vs z 

- For +ve β , as z is decreasing to the limit 0, effective ω_d becomes +ve to -ve.

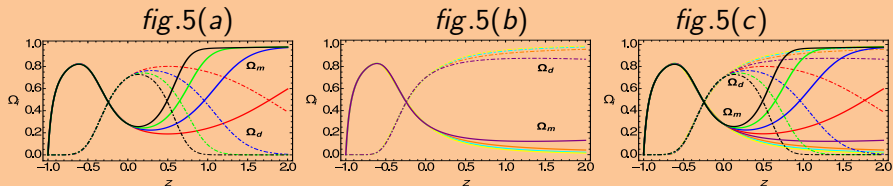
EoS vs z 

- For +ve β , as z is decreasing to the limit 0, effective ω_d becomes +ve to -ve.
- At $z = 0$ these curves are $\dot{\omega}_d$ or $\dot{D} = -1$ and decrease as we move towards the $z = -1$ value. If β is -ve, the ω_d stays -ve always.

EoS vs z 

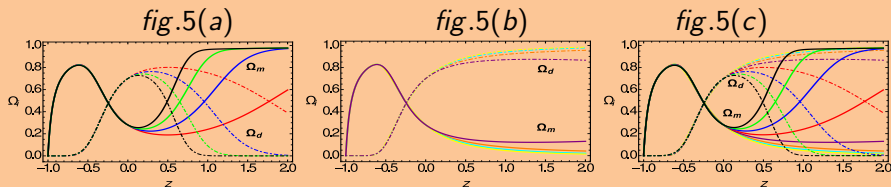
- For +ve β , as z is decreasing to the limit 0, effective ω_d becomes +ve to -ve.
- At $z = 0$ these curves are $\dot{\omega}_d$ or $\dot{D} = -1$ and decrease as we move towards the $z = -1$ value. If β is -ve, the ω_d stays -ve always.
- Except $\beta = 0.5$ case, all other the rate of changes in the DE EoS +ve cases are decreasing as z is decreasing. As we choose β to be -ve, $d\omega_d$ is found to be increasing with decreasing z .

$$\Omega_{i_0} = \frac{8\pi G}{3H_0^2} \rho_{i_0}, \quad i = rad, m, d$$



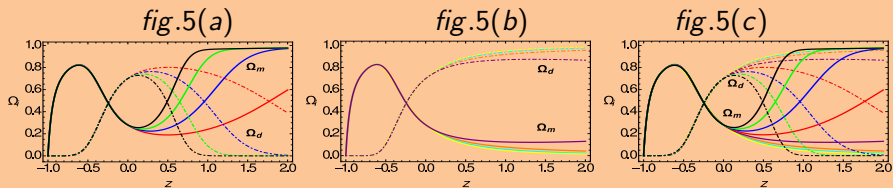
- If redshift is -ve, the dimensionless densities fall to vanish in future infinity.

$$\Omega_{i_0} = \frac{8\pi G}{3H_0^2} \rho_{i_0}, \quad i = rad, m, d$$



- If redshift is -ve, the dimensionless densities fall to vanish in future infinity.
- To justify, we may suggest that some unknown matter density is involved in future. As this has not theoretically been incorporated, the sum of the mass fraction falls.

$$\Omega_{i_0} = \frac{8\pi G}{3H_0^2} \rho_{i_0}, \quad i = rad, m, d$$



- If redshift is -ve, the dimensionless densities fall to vanish in future infinity.
- To justify, we may suggest that some unknown matter density is involved in future. As this has not theoretically been incorporated, the sum of the mass fraction falls.
- For +ve β , it is observed that in the past Ω_m dominated Ω_d and in the recent past the opposite happened. If β is -ve, Ω_d dominates all over the +ve domain of redshift.

Deceleration Parameter

we study deceleration parameter given as,

$$q = -\frac{\ddot{a}}{aH^2} = -\left(1 + \frac{\dot{H}}{H^2}\right), \quad (7)$$

where $\dot{H} = \frac{dH}{dt} = aH \frac{dH}{da}$. For our study, q is expressed as

$$q = \frac{a^{3(\omega_0 + \frac{\omega_1}{\beta})} \beta (a\Omega_{m0} + 2\Omega_{rad0}) + a \exp\left\{\frac{3(a^\beta - 1)\omega_1}{\beta^2}\right\} \Omega_{d0} \left\{ \beta(1 + 3\omega_0) - 3\omega_1(a^\beta - 1) \right\}}{2\beta \left\{ a \exp\left\{\frac{3(a^\beta - 1)\omega_1}{\beta^2}\right\} \Omega_{d0} + a^{3(\omega_0 + \frac{\omega_1}{\beta})} (a\Omega_{m0} + \Omega_{rad0}) \right\}}$$

Deceleration Parameter Graphs

fig.6(a)

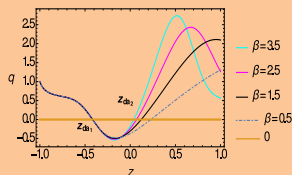


fig.6(b)

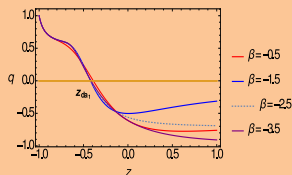
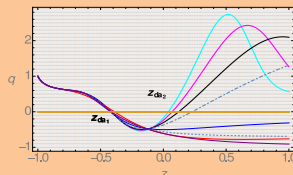


fig.6(c)



- For +ve β , we observe a deceleration in the past, then through a phase transition accelerating era begins and again in future, a decelerating era begins and again in future, a decelerating phase is predicted to obtain.

Deceleration Parameter Graphs

fig.6(a)

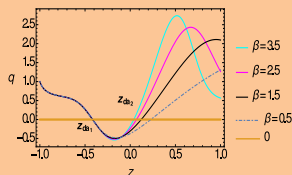


fig.6(b)

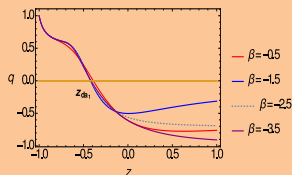
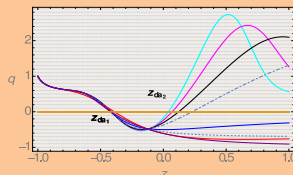


fig.6(c)



- For +ve β , we observe a deceleration in the past, then through a phase transition accelerating era begins and again in future, a decelerating era begins and again in future, a decelerating phase is predicted to obtain.
- Much interesting result is found to obtain for -ve β cases. An acceleration is seen in the past and even at present time. However, in future a deceleration is expected to take place.

Statefinder Parameter $\{r, s\}$

Next we study the variations of statefinder parameters r and s . The statefinder parameters [2] are described as,

$$r = \frac{\ddot{a}}{aH^3} \quad (8)$$

$$s = \frac{r - 1}{3(q - \frac{1}{2})}, \quad (9)$$

where a , \ddot{a} , H , q are the scale factor of the universe, third order differentiation with respect to the cosmic time t , the Hubble parameter and the deceleration parameter respectively.

Statefinder Parameter Graphs

fig.7(a)

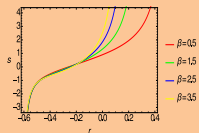


fig.7(b)

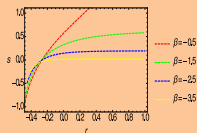


fig.7(c)

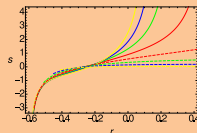


fig.8(a)

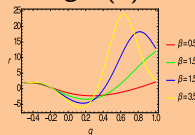


fig.8(b)

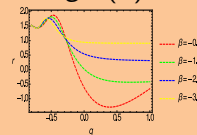
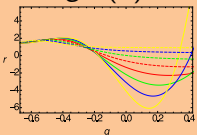


fig.8(c)



Statefinder Parameter Graphs

fig.7(a)

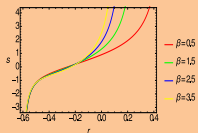


fig.7(b)

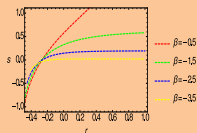


fig.7(c)

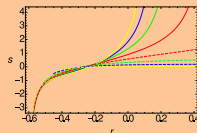


fig.8(a)

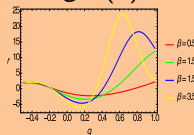


fig.8(b)

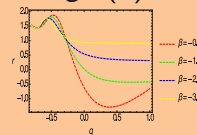
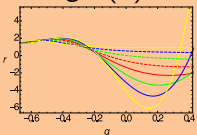


fig.8(c)



We plot s vs r in the figures 7(a)-(c). For all the cases the curves are increasing for increasing r . r vs q graphs have been plotted in figures 8(a)-(c). The graphs are found to be enhanced periodically. It is observed that infinite jumps are possible.

In a nutshell

- First we have constrained the free parameters of the model with a Hubble parameter vs redshift dataset accompanied with baryon acoustic oscillations and cosmic microwave background tools. Differential ages method is used to collect forty six data points.

In a nutshell

- First we have constrained the free parameters of the model with a Hubble parameter vs redshift dataset accompanied with baryon acoustic oscillations and cosmic microwave background tools. Differential ages method is used to collect forty six data points.
- As we increase negativity of β , the major axis of the confidence contours rotate with a +ve angle in the $\omega_0 - \omega_1$ plane. This means if negativity of β increases, low ω_0 high ω_1 values are accepted to stay constrained with the chosen dataset. Negativity of β constrains the parameters more in a shorter confidence region.

In a nutshell

- First we have constrained the free parameters of the model with a Hubble parameter vs redshift dataset accompanied with baryon acoustic oscillations and cosmic microwave background tools. Differential ages method is used to collect forty six data points.
- As we increase negativity of β , the major axis of the confidence contours rotate with a +ve angle in the $\omega_0 - \omega_1$ plane. This means if negativity of β increases, low ω_0 high ω_1 values are accepted to stay constrained with the chosen dataset. Negativity of β constrains the parameters more in a shorter confidence region.
- Combined study of the parameters show that the best fits are likely to be different. Analysis shows that when β is high, ω_1 can take a larger span and for ω_0 and β the scenario is just the opposite.

In a nutshell

- First we have constrained the free parameters of the model with a Hubble parameter vs redshift dataset accompanied with baryon acoustic oscillations and cosmic microwave background tools. Differential ages method is used to collect forty six data points.
- As we increase negativity of β , the major axis of the confidence contours rotate with a +ve angle in the $\omega_0 - \omega_1$ plane. This means if negativity of β increases, low ω_0 high ω_1 values are accepted to stay constrained with the chosen dataset. Negativity of β constrains the parameters more in a shorter confidence region.
- Combined study of the parameters show that the best fits are likely to be different. Analysis shows that when β is high, ω_1 can take a larger span and for ω_0 and β the scenario is just the opposite.
- We observe that the best fits for positive β cases are pointed towards nearly -1 values at the present epoch. So we conclude Λ CDM is supported with zero redshift or present time. It is followed for positive β as z reduces curves and the rate of decrease changes at $z = 0$.

- We observe, however, that our prediction with BAZS at $z = 0$ that the EoS will have a value a little lower than -1. When we add a BAO constrain along with the enlist OHD. This fact is more prominent.







- We observe, however, that our prediction with BAZS at $z = 0$ that the EoS will have a value a little lower than -1. When we add a BAO constrain along with the enlist OHD. This fact is more prominent.
- Early universe shows the matter density to dominate over dark energy density.

- We observe, however, that our prediction with BAZS at $z = 0$ that the EoS will have a value a little lower than -1. When we add a BAO constrain along with the enlist OHD. This fact is more prominent.
- Early universe shows the matter density to dominate over dark energy density.
- We observe that a future deceleration is possible for both of β positive and negative cases. Even after being positive.

- We observe, however, that our prediction with BAZS at $z = 0$ that the EoS will have a value a little lower than -1. When we add a BAO constrain along with the enlist OHD. This fact is more prominent.
- Early universe shows the matter density to dominate over dark energy density.
- We observe that a future deceleration is possible for both of β positive and negative cases. Even after being positive.
- q turns to be a finite valued function. This makes this model special to be studied alongside CPL, Λ CDM and other redshift dependent EoSs.

- We observe, however, that our prediction with BAZS at $z = 0$ that the EoS will have a value a little lower than -1. When we add a BAO constrain along with the enlist OHD. This fact is more prominent.
- Early universe shows the matter density to dominate over dark energy density.
- We observe that a future deceleration is possible for both of β positive and negative cases. Even after being positive.
- q turns to be a finite valued function. This makes this model special to be studied alongside CPL, Λ CDM and other redshift dependent EoSs.

References

-  Barboza, Jr., E. M., Alcaniz, J. S., Zhu, Z.-H., & Silva, R. :- *Phys. Rev. D*, **80**, 043521 (2009).
-  Sahni, V., Saini, T. D., Starobinsky, A. A., Alam, U. :- *JETP Lett.*, **77**, (2003) 201-206; *Pisma Zh. Eksp. Teor. Fiz.*, **77**, 249-253 (2003).
-  Hicken, M et al. :- *Astrophys. J.*, **700**, 1097 (2009).
-  Efstathiou, G. :- *Mon. Not. R. Astron. Soc.*, **310**, 842 (1999)
arXiv:astro-ph/9904356v1.
-  Perlmutter, S., Aldering, G., Goldhaber, G. et al. :- “Measurements of Omega and Lambda from 42 High-Redshift Supernovae”, *Astrophys. J.*, **517**, (1999) [arXiv:astro-ph/9812133].
-  Riess A. G., Filippenko, A. V., Challis, P. et al., “Observational Evidence from Supernovae for an Accelerating Universe and a Cosmological Constant” , *Astron. J.*, **116**, (1998) 1009
[arXiv:astro-ph/9905126]

Thank
you

